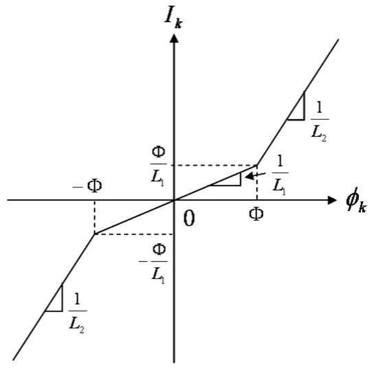

Fig. 2. $\phi - i$ charactristics of the nonlinear inductor.

Fig. 2 is described as following function.

$$I_k = \frac{\phi_k}{L_2} + \left(\frac{1}{L_1} - \frac{1}{L_2}\right)\frac{|\phi_k + \Phi| - |\phi_k - \Phi|}{2}. \tag{2}$$

By changing the variables and parameters,

$$\begin{aligned} &t = \sqrt{L_1 C}\,\tau, \quad a = \sqrt[8]{r_d\sqrt{\frac{C}{L_1}}}, \quad \text{“}\cdot\text{”} = \frac{d}{d\tau}, \\ &\phi_k = a\sqrt{L_1 C}\,x_k, \quad i_k = a\sqrt{\frac{C}{L_1}}\,y_k, \quad v_k = a\,z_k, \\ &\alpha = \frac{L_1}{L_0}, \quad \beta = r\sqrt{\frac{C}{L_1}}, \quad \gamma = \frac{L_2}{L_0}, \quad \delta = \frac{\Phi}{a\sqrt{L_1 C}}. \end{aligned} \tag{3}$$

the circuit equations are normalized and described as

$$\begin{aligned} \dot{x}_1 = \frac{1}{1+m_1-2m_1m_2}\Bigg(&\frac{1-m_1m_2}{1-m_1}\{\beta(X_1+y_1)-z_1\} \\ &- \frac{m_1(1-m_2)}{1-m_1}\{\beta(X_2+y_2)-z_2\} \\ &- m_2\{\beta(X_3+y_3)-z_3\}\Bigg) \\ \dot{x}_2 = \frac{1}{1+m_1-2m_1m_2}\Bigg(&\frac{1-m_1m_2}{1-m_1}\{\beta(X_2+y_2)-z_2\} \\ &- \frac{m_1(1-m_2)}{1-m_1}\{\beta(X_1+y_1)-z_1\} \\ &- m_2\{\beta(X_3+y_3)-z_3\}\Bigg) \\ \dot{x}_3 = \frac{1}{1+m_1-2m_1m_2}\Bigg(&(1+m_1)\{\beta(X_3+y_3)-z_3\} \\ &- m_1\{\beta(X_1+y_1)-z_1\} \\ &- m_1\{\beta(X_2+y_2)-z_2\}\Bigg) \\ \dot{y}_k = \alpha\{\beta(X_k+y_k) &- z_k - f(y_k)\} \\ \dot{z}_k = X_k + y_k & \qquad\qquad (k = 1,2,3) \end{aligned} \tag{4}$$

where

$$\begin{aligned} X_k &= \frac{\alpha}{\gamma}x_k + \left(1 - \frac{\alpha}{\gamma}\right)\frac{|x_k+\delta| - |x_k-\delta|}{2}. \\ f(y_k) &= \sqrt[9]{y_k}. \end{aligned} \tag{5}$$

III. COMPUTER CALCULATED RESULTS

In this section, we perform computer calculations for some cases. First, we consider the case where parameter m_1 is much larger than parameter m_2. In this case, one subcircuit is not easy to interact with the other subcircuits. Next, the case where parameter m_1 is almost equal to parameter m_2 is considered. All subcircuits dominantly interact in this case. The parameter values corresponding to the inductors are fixed as α = 20.0, γ = 10.0 and (4) is calculated by using the Runge-Kutta method with step size Δt = 0.001.

A. Case for $m_1 \gg m_2$

We set the parameter values $m_1 = 0.2$ and $m_2 = 0.02$ in this case. Subcircuit 3 is not easy to interact with subcircuits 1 and 2. Therefore subcircuit 3 becomes asynchronous to the others.

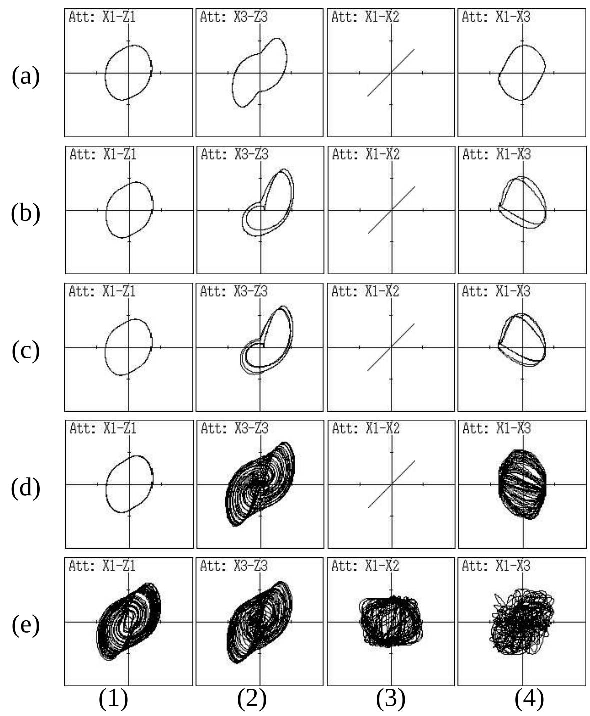

Fig. 3. In-phase synchronization for case A. m_1 = 0.2. m_2 = 0.02. δ = 0.5. (a) β = 0.15. (b) β = 0.18. (c) β = 0.181. (d) β = 0.2. (e) β = 0.23. (1) x_1 vs. z_1. (2) x_3 vs. z_3. (3) x_1 vs. x_2. (4) x_1 vs. x_3.

Figure 3 shows the in-phase synchronization and the asynchronous state. From Figs. 3(1) and (3), we can confirm that the attractors observed from subcircuit 1 and 2 bifurcate to chaotic attractors keeping in-phase synchronization (a)-(d). While, the attractor observed from subcircuit 3 bifurcates to chaotic attractor via period-doubling route Figs. 3(2)(a)-(e). In

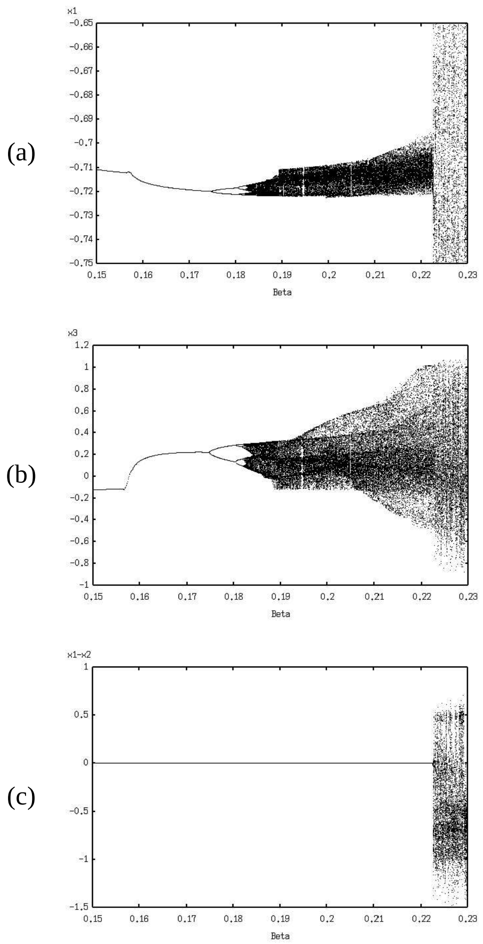

Fig. 4. Bifurcation diagram for the in-phase synchronization. m_1 = 0.2. m_2 = 0.02. δ = 0.5. (a) Horizontal: β. Vertical: x_1. (b) Horizontal: β. Vertical: x_3. (c) Horizontal: β. Vertical: $x_1 - x_2$.

order to investigate the bifurcation route in detail, we made one-parameter bifurcation diagrams. The poincare section is defined as z_1 = 0, $x_1 < 0$. Figure 4 shows the bifurcation diagram for in-phase synchronization. From these figures, we can confirm the bifurcation route via period-doubling. We can also confirm that breakdown of chaos synchronization around $\beta = 0.223$ from Fig. 4(c).

Next, we also investigate the anti-phase synchronization by changing the initial values. Figures 5(a) and (b) shows the anti-phase synchronization for subcircuit 1 and 2. While, the attractors observed from subcircuit 3 become asynchronous state. Figure 6 shows bifurcation diagram for anti-phase synchronization. As parameter β increases, the anti-phase synchronization becomes unstable and the in-phase synchronization is observed around $\beta = 0.2$ as Fig. 5(3)(c) and Fig. 6.

B. Case for $m_1 \approx m_2$

In this case, we set the parameter values $m_1 = 0.2$ and $m_2 = 0.19$. Therefore, subcircuit 3 is easy to interact subcircuit 1 and 2.

First, we investigate the in-phase synchronization. Figure 7 shows that all subcircuits are synchronized at in-phase. However as β increases, the in-phase synchronization becomes unstable and breaks down (c),(d).

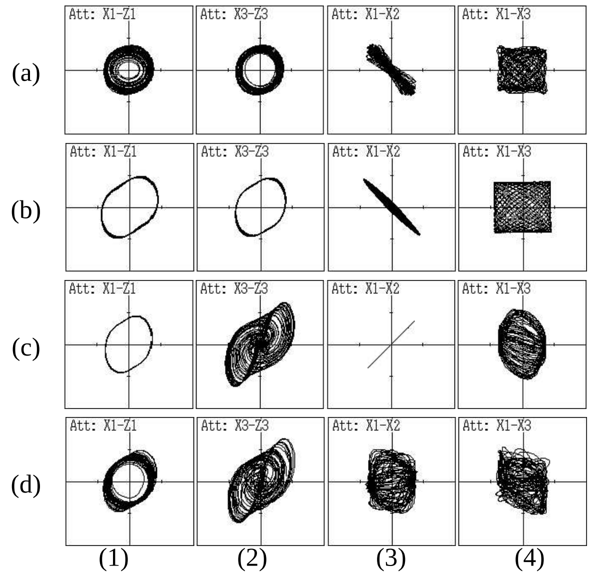

Fig. 5. Anti-phase synchronization for case A. m_1 = 0.2. m_2 = 0.02. δ = 0.5. (a) β = 0.02. (b) β = 0.18. (c) β = 0.2. (d) β = 0.23. (1) x_1 vs. z_1. (2) x_3 vs. z_3. (3) x_1 vs. x_2. (4) x_1 vs. x_3.

Next, the three-phase synchronization is observed by changing the initial values. Figure 8 shows the three-phase synchronization. From this figure, we can confirm that each one-periodic attractor (a) bifurcates to torus (b), and as β increases, the torus bifurcates to chaos (c) and the chaos grows as (d). Figure 9 shows bifurcation diagram of the three-phase synchronization. We can confirm that the bifurcation route of the three-phase synchronization from Fig. 9, namely bifurcation of the one-periodic solution to torus around β = 0.203, the generation of chaotic solution for β values more than 0.215 and the generation of periodic solution around β = 0.225.

IV. CONCLUSIONS

In this research, we investigated quasi-synchronization phenomena observed from simple chaotic circuits with asymmetric coupling by nonlinear mutual inductors. By carrying out the computer calculations, we confirmed that various quasi-synchronization phenomena of chaos were observed.

In the future, we investigate phenomena observed from the case which four or more subcircuit are coupled asymmetrically by nonlinear mutual inductors.

REFERENCES

[1] Y. Nishio and A. Ushida, "Spatio-Temporal Chaos in Simple Coupled Chaotic Circuits," IEEE Trans. on Circuit and Systems-I, vol. 42, no. 10, pp. 678.686, Oct. 1995.

[2] J.A.K. Suykens, P.F. Curran and L.O. Chua, "Master-Slave Synchronization Using Dynamic Output Feedback," International Journal of Bifurcation and Chaos, vol. 7, no. 3, pp. 671-679. 1997.

[3] M. Wada, Y. Nishio and A. Ushida, "Analysis of Bifurcation Phenomena in Two Chaotic Circuits Coupled by an Inductor," IEICE Transactions on Fundamentals, vol. E80-A, no. 5, pp. 869-875, May 1997.

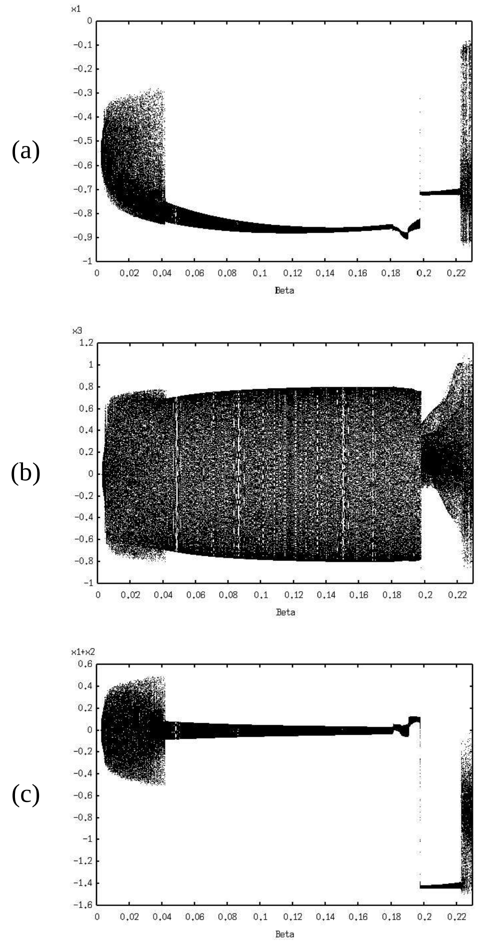

Fig. 6. Bifurcation diagram for the anti-phase synchronization. m_1 = 0.2. m_2 = 0.02. δ = 0.5. (a) Horizontal: β. Vertical: x_1. (b) Horizontal: β. Vertical: x_3. (c) Horizontal: β. Vertical: $x_1 + x_2$.

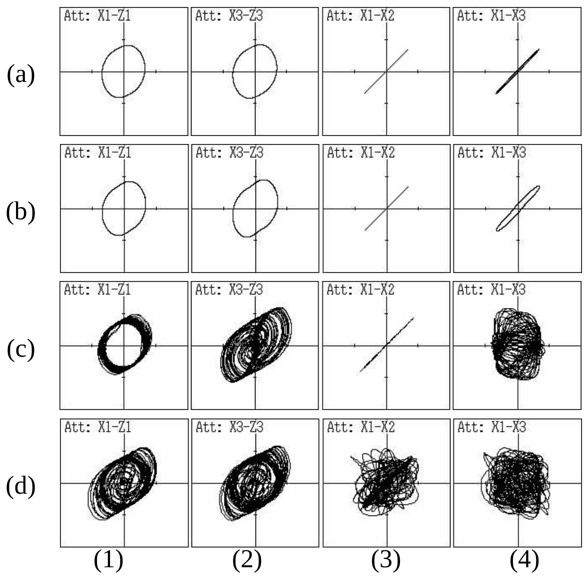

Fig. 7. In-phase synchronization for case B. m_1 = 0.2. m_2 = 0.19. δ = 1.5. (a) β = 0.15. (b) β = 0.23. (c) β = 0.26. (d) β = 0.27. (1) x_1 vs. z_1. (2) x_3 vs. z_3. (3) x_1 vs. x_2. (4) x_1 vs. x_3.

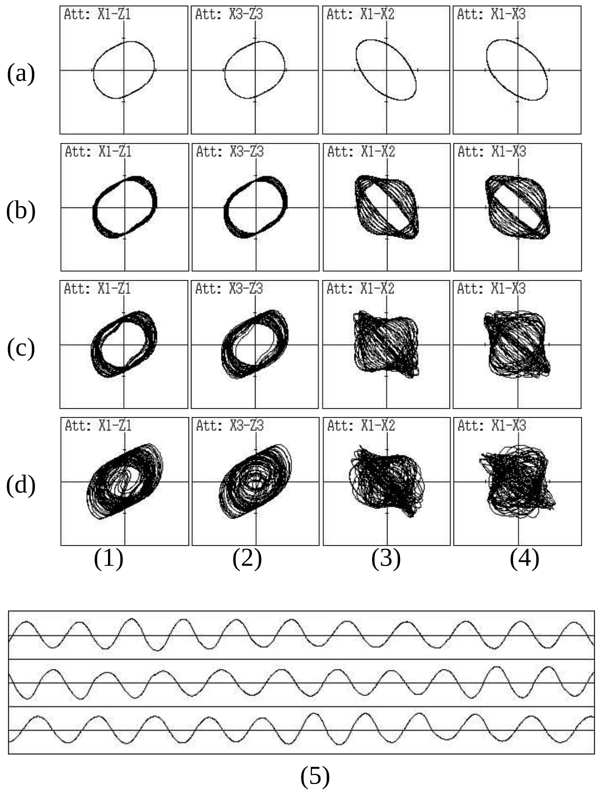

Fig. 8. Three-phase synchronization for case B. m_1 = 0.2. m_2 = 0.19. δ = 1.5. (a) β = 0.15. (b) β = 0.2. (c) β = 0.22. (d) β = 0.24. (1) x_1 vs. z_1. (2) x_3 vs. z_3. (3) x_1 vs. x_2. (4) x_1 vs. x_3. (5) Time waveform for β = 0.22.

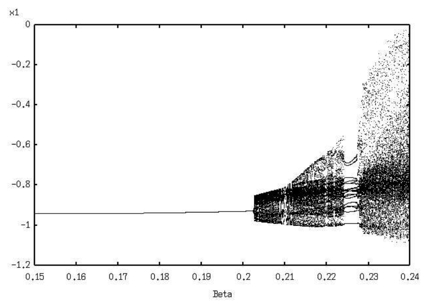

Fig. 9. Bifurcation diagram for the three-phase synchronization. m_1 = 0.2. m_2 = 0.19. δ = 1.5. Horizontal: β. Vertical: x_1.

[4] G.O. Zhong, C.W. Wu and L.O. Chua, "Torus-Doubling Bifurcations in Four Mutually Coupled Chua's Circuits," IEEE Transactions on Circuits and Systems I, vol. 45, no. 2, pp. 186-193. 1998.
[5] I.P. Marino, V. Perez-Munuzuri and M.A. Matias, "Desynchronization Transitions in Rings of Coupled Chaotic Oscillators," International Journal of Bifurcation and Chaos, vol. 8, no. 8, pp. 1733-1738. 1998.
[6] Y. Komatsu, Y. Uwate and Y. Nishio, "Synchronization in Chaotic Circuits Coupled by Mutual Inductors," Proc. of NCSP'06, pp. 293-296, Mar. 2006.
[7] N. Inaba and S. Mori, "Chaotic Phenomena in Circuits with a Linear Negative Resistance and an Ideal Diode," Proc. of MWSCAS'88, Aug. 1988, pp. 211-214.